Progress towards a space-borne quantum gravity gradiometer

Nan Yu, James M. Kohel, Jaime Ramerez-Serrano, James R. Kellogg, Lawrence Lim and Lute Maleki
Jet Propulsion Laboratory
California Institute of Technology
4800 Oak Grove Drive, Pasadena, CA 91109

Abstract— **Quantum interferometer gravity gradiometer for 3D mapping is a project for developing the technology of atom interferometer-based gravity sensor in space. The atom interferometer utilizes atomic particles as free fall test masses to measure inertial forces with unprecedented sensitivity and precision. It also allows measurements of the gravity gradient tensor components for 3D mapping of subsurface mass distribution. The overall approach is based on recent advances of laser cooling and manipulation of atoms in atomic and optical physics. Atom interferometers have been demonstrated in research laboratories for gravity and gravity gradient measurements. In this approach, atoms are first laser cooled to micro-kelvin temperatures. Then they are allowed to freefall in vacuum as true drag-free test masses. During the free fall, a sequence of laser pulses is used to split and recombine the atom waves to realize the interferometric measurements. We have demonstrated atom interferometer operation in the Phase I period, and we are implementing the second generation for a complete gradiometer demonstration unit in the laboratory. Along with this development, we are developing technologies at component levels that will be more suited for realization of a space instrument. We will present an update of these developments and discuss the future directions of the quantum gravity gradiometer project.**

I. Introduction

Gravity field mapping is one of the key measurements required in order to understand the solid earth, ice and oceans, and dynamic processes in a comprehensive model of our planet. There have been a number of gravity measurement missions such as CHAMP and GRACE [1]. These missions use satellites themselves as test masses and measure the gravity through the precise monitoring of the motion of the satellites. Other gravity missions using mechanical gravity gradiometers have also been planned or under study [2], [3]. The recent advent of laser cooling and manipulation of atoms has lead to an entirely new class of gravity sensors: quantum gravity gradiometer (QGG) based on atom interferometer. Unlike any previously known gravity sensors, the quantum gravity gradiometer uses atoms themselves as drag-free test masses. At the same time, the quantum wave-like nature of atoms is utilized to carry out interferometric measurement of the effect of gravity on the atoms. The exquisite sensitivity potentially achievable with atom-wave interferometry holds great promise for new gravity mapping and monitoring capabilities — higher measurement sensitivity, finer spatial resolution, and temporal monitoring. All these will provide new gravity measurement opportunities for the Earth Observing System in understanding the planetary inner structure and dynamics, changes in ice sheets and ocean currents, changes in underground water storage, and in overall scientific geodesy study.

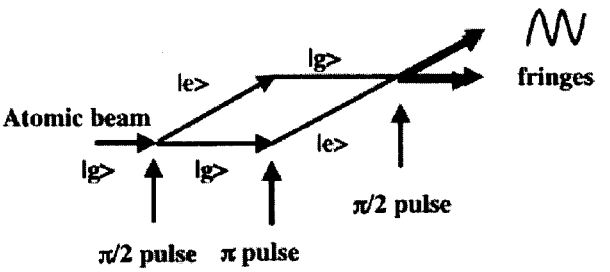

Fig. 1. Illustration of a March-Zehnder atom interferometer with light pulsed as atom wave optics.

In this paper, we will review briefly the principles of the quantum gravity gradiometer and its advantages in space environment. We will then describe our laboratory experiment and report some of the component development work towards a space-borne system.

II. Atom Interferometer Gravity Gradiometer

The fundamental concept of atom interferometry and its use as inertial sensors have been described in the literature [4]–[7]. Briefly, one exploits the wave-like nature of atoms to construct an atom interferometer analogous to laser interferometers. One of the approaches to the atom wave beam splitting and recombining is using light pulses [4], as shown in Fig. 1. To understand this approach, one is reminded that photons carry momentum. When an atom absorbs/emits a photon, its momentum changes accordingly. Therefore, one starts with a $\pi/2$ laser pulse that puts the atom in an equal superposition of the ground and excited states. While the excited state of the atom changes its momentum due to the photon absorption, the ground state remains unchanged, thus accomplishing the atom wave beam splitting. Similarly, a π-pulse exchanges the states, functioning as a mirror in redirecting the atom wave. Therefore, a sequence of $\pi/2$-π-$\pi/2$ pulses makes up a Mach-Zehnder type inteferometer as shown in Fig. 1.

In the absence of the gravity, the two paths of the interferometer arms would be identical and no relative phase shifts result. If, on the other hand, atoms experience an acceleration g during this time, a net phase difference is accumulated. This phase difference can be shown to be $\Delta\phi = kgT^2$, where the

interrogation time T is the time between the light pulses, and k is the effective laser wave number [4]. It is clear in the picture described above that the atom internal states have one-to-one correspondence to the paths of the atom beam. Therefore, the fringe of the interferometer can be read out by monitoring the relative populations of the two states in the recombined atoms via laser-induced fluorescence. Knowing the laser wave number and the interrogation time, the gravity acceleration g can be determined.

To see the resulting sensitivity in this kind of device, let's consider Cs atoms with a transition wavelength of 852 nm: with 1 s interrogation time, a mere $7 \times 10^{-9} g$ of the gravity acceleration will cause a fringe phase shift of one full radian in a single measurement. The overall measurement sensitivity will depend on the readout signal-to-noise ratio (SNR), which is primarily determined by the atom number shot noise. A shot-noise-limited SNR greater than 1000 per atom launch has been demonstrated [8]. This would imply a sensitivity better than $10^{-11} g$ for $T = 1$ s.

Although the gravitational acceleration can be measured directly as described above, this measurement requires an inertial frame of reference which is very difficult to realize even in a controlled laboratory environment. This difficulty roots to Einsteins Equivalence Principle, which states that one cannot distinguish the reference frame acceleration from the gravitational acceleration in a local measurement. Gravity gradiometry then provides a more fundamental measure of the gravitational field. A gradiometer measures the gravitational acceleration difference between two locations with a common reference frame. Other inertial accelerations will be rejected as common mode noise. The simplest implementation of a QGG consists of two atom-interferometer accelerometers separated by some distance. The two acceleration measurements are performed simultaneously and by using the same atom interferometer laser beams, so that the common-mode noise and uncertainties are effectively cancelled [9], as illustrated in Fig. 2. With this configuration in a laboratory setting, a gravity gradient sensitivity of 10 E/Hz$^{1/2}$ (gravity gradient unit 1 E $= 10^{-9}$ s^{-2}) has been demonstrated with an effective common-mode rejection of 140 dB [9].

Impressive as the laboratory demonstrations were, the most significant sensitivity gain can come from the operation of an atom interferometer gravity gradiometer in space. As discussed before, the gradiometer sensitivity increases with the square of the interrogation time, in contrast to the $1/T$ increase in precision with most other precision measurements such as atomic clocks. In a ground-based experiment in an atomic fountain, the interrogation time is limited to a fraction of a second due to practical limitations in the height of the apparatus. When operating a similar experiment in a microgravity environment, the atoms will be truly drag-free. This allows interrogation times much longer, and accordingly an inertial sensing sensitivity much higher than that is possible on the ground.

When the interrogation time becomes too long, one starts to lose the number of atoms due to the finite temperature of the cold atom cloud. The atom cloud volume expands as T^3. In the worse case of the atom loss limit, the SNR goes down as

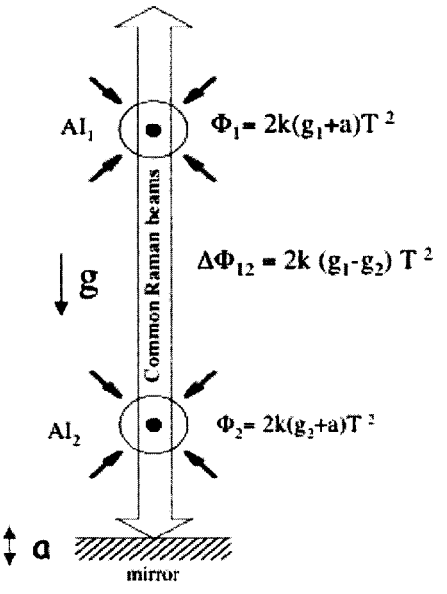

Fig. 2. Illustration of two magneto-optical traps and the configuration as a gravity gradiometer. The small shaded arrows designate the counter-propagating MOT beams with the dots as trapped atom clouds. They share the same Raman laser beams for high common-mode noise rejection

$T^{-3/2}$. As a result, the phase shift for a given acceleration goes as $T^{1/2}$. In other words, one continues to gain the sensitivity by going to longer interrogation time even as one loses the number of atoms. Laser cooling can reduce the atom temperature to about 2 μK, which corresponds to a mean atom velocity of 2 cm/s. For example, a 10 s interrogation time in space with a modest SNR of 100 will have $10^{-13} g$ in a single measurement sequence of the accelerometer. A gradiometer with a baseline separation of 10 m would give a corresponding sensitivity about 3×10^{-4} E per single measurement, or roughly 0.001 E/Hz$^{1/2}$.

To recover any three-dimensional information about the mass distribution, it is necessary to measure multiple tensor components of the gravity. In the microgravity environment, the absence of the large gravitational bias makes the atom interferometer operation similar in all directions. Therefore, similar gradient measurement sensitivities can be obtained in all directions. However, the atom interferometer is affected by rotation. An orbiting satellite will always have rotations in the plane of the orbit. Only the direction perpendicular to the orbital plane can be free from rotation. This means that the noises from rotations are not the same for all directions. The effects of the rotation and mitigations are currently under study.

III. Instrument Development

In our quantum gravity gradiometer, the light-pulse atom interferometer technique is used. The cesium atoms are first collected and cooled by lasers into a small cloud in a magneto-optic trap (MOT). The MOT, consisting of three pairs of counter-propagating laser beams along three orthogonal axes centered on a non-uniform magnetic field, collects up to 10^{10}

atoms from a beam or a background vapor. After these atoms are collected, further laser-cooling brings the atoms temperature down to micro Kelvins. The cold atoms are launched vertically by introducing a slight frequency shift between pairs of lasers to create a moving frame for the atom ensemble. This so-called "atomic fountain" allows us twice the available interaction time with the atoms in an apparatus of a given height. The atom interferometry is then performed during the subsequent free fall of atoms in the atomic fountain.

We have been developing a ground-based atom interferometer gravity gradiometer system with the goal towards producing a portable and eventually a space-flyable system. There are three major subsystems of the gradiometer: the atomic physics package, the laser system, and the control system.

The atomic physics package is centered with an ultra-high vacuum enclosure where atoms are collected, cooled, and interrogated. We have had a vacuum system with mostly off-the-shelf parts as our test beds. With this system, we have demonstrated the atom interferometer fringes [7]. We have recently designed and acquired an all-titanium vacuum enclosure with welded optical windows. This enclosure was designed to offer the flexibility and allows a comprehensive system requirement study. In this new physics package, we will also use a new compact cold atom source for loading the atoms to the UHV MOT rather than collecting the atoms from the background pressure as we have done in the past.

In the following sections, we will report in detail three subsystem developments. There are the compact cold atom source, the modular laser system, and the laser frequency and phase locking.

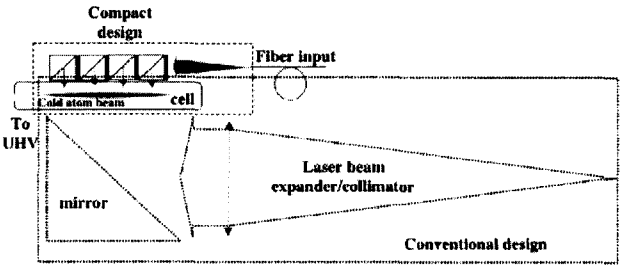

Fig. 3. The illustration shows that large optics are required in conventional 2D MOT configurations as indicated in the dotted lines below the atom cell. Above the cell, the new optics arrangement with multi-state MOT considerably reduces the overall size and the profile of the source.

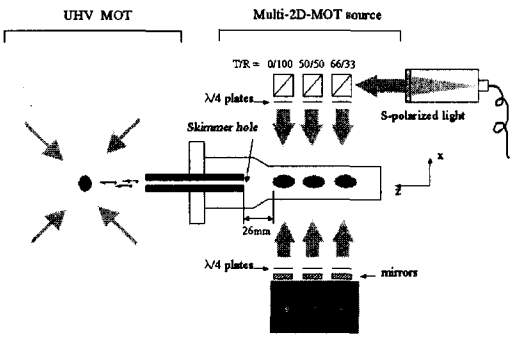

Fig. 4. Schematic of the experimental apparatus, including the multiple 2D-MOT source of cold atoms and UHV MOT. The separations of the splitter cubes and the distances to the cell are exaggerated for clarity. Also shown in the figure are the laser beam profiles.

A. Compact cold atom source

In our previous atomic fountain, atoms were collected from the background vapor pressure. It is difficult to optimize system performance with this approach. A high vapor pressure is needed for fast loading of atoms but it causes collisions and also large background signals at detection. A solution to this dilemma is to use a separate high-flux atom source for loading the magneto-optical trap (MOT) in ultra-high vacuum (UHV). This allows one to achieve a high loading rate of the UHV MOT while keeping the background pressure low. While there have been several distinct approaches of cold sources, a 2D MOT source from a higher pressure vapor cell is the simplest and most effective for alkaline atoms [10]. In a conventional 2D MOT configuration, however, the length of the 2D MOT determines the laser beam size needed as illustrated in Fig. 3. The overall volume of the optics package becomes correspondingly large, making the 2D source a very bulky addition to the setup.

We have designed a new configuration of compact cold beam source. The device consists of multiple stages of 2D MOTs. Each individual MOT is short in length, requiring a correspondingly small laser beam size. A chain of such small MOTs is used to achieve a total high flux, while the overall size of the atom source is significantly reduced compared to the conventional single 2D MOT of a similar length. It also requires no in-vacuum optics. The overall design is compact, simple, and robust.

The experimental setup is shown in Fig. 4. The beam source consists of a series of short (12.7 mm-long) 2D-traps along the centerline of a two-dimensional quadrupole magnetic field produced by a hairpin coil. In the middle is a small Cs vapor cell that is attached to the UHV chamber through a glass-to-metal seal. The cell is 45 mm long with a 12 mm square cross section. The pressure difference between the source and UHV regions is maintained through a differential pumping tube of 4 mm aperture. Inside the tube is a series of graphite getters. To reduce the cold atom flux collisional loss through the high pressure region before entering UHV chamber, the differential pumping tube is extended close to the 2D MOT. As will be seen later, this extraction arrangement proves effective when the source is operating at a high vapor pressure.

Each individual 2D MOT is formed by a pair of retro-reflected laser beams formed by a beam splitting cube and the retro-reflecting mirror. Quarter wave plates are inserted in front of each beam splitter and mirror to produce the desired $\sigma^+ - \sigma^-$ polarization for the 2D MOT operation. A collimated laser beam of 10 mm $1/e^2$ diameter is sent in from the side parallel to the atom beam direction. The collimated beam passing through a series of beam splitters with the appropriate splitting ratios such that all MOTs have approximately equal powers. With this arrangement, the laser beam profile along

the cell is a series of the truncated gaussian beams. We chose to use the simple AR-coated nonpolarizing beam splitters since the splitting ratio is not critical. The size of the beam splitting cubes are 12.7 mm, matching the cell size. The cubes are placed next to each other. This multiple 2D MOT arrangement eliminates the need for large cylindrical optics. The laser beam diameter is about the size of the beam splitting cube and is independent of the overall length of the 2D MOT source. The entire source setup, including all the 2D MOT optics and the laser collimators can fit into a 4×4 cm^2 cylindrical shell with only fiber optics and magnetic coil input connections.

We have optimized the operation of the multi-stage 2D MOT as the cold atom source. The optimization was done mainly respective to the laser intensity, detuning, and the operating vapor pressure. We have found that the operation of the multiple 2D MOTs is similar to that of a single stage 2D MOT with the comparable length [10]. There exits an optimal laser detuning for a given magnetic field gradient of the 2D MOT. With 5 G/cm field used, we found the flux peaked at about 1.4Γ, where Γ is the Cs transition linewidth. In the low laser intensity limit, the flux increases with the increasing laser intensity. In addition, the optimal operating vapor pressure depends on the length of the MOT. A longer 2D MOT tends to give a higher flux at a lower vapor pressure. This clearly indicates the collision loss effect. A detailed description of the multi-stage MOT source will be published elsewhere [11].

We have operated the compact source using up to 5 stages. The total flux increases with the number of stages N with a scale factor about $N^{1.2}$. With the 5-stage setup, we have obtain a total flux of 1.4×10^9 atom/s with only 15 mW of total trapping laser input power. Depending on the number of stages used in the 2D-MOT source, the mean velocity of the beam varies from 21 m/s for the single stage system to 38 m/s for the 5-stage configuration with the full width half maximum as little as 10 m/s. The low velocity of the atoms from the source can be captured with a small UHV MOT about 3 cm in diameter. A much higher flux can be obtained with higher input laser powers.

B. Modular laser and optics system

The entire measurement process of the atom interferometer device relies heavily on laser interactions with atoms. Therefore, the laser requirement is demanding, requiring more than 20 separate laser beams with both intensity and frequency controls. We have developed a compact and robust laser and optics system with functional modules as building blocks. This system reduced the laboratory optics setup spread over a large optical table into two $2' \times 3'$ breadboard boxes. The modules are interconnected using optics fibers.

In addition to the size, small module approach also improves the alignment stability. Instabilities are typically caused by misalignments due to mechanical and thermal effects. The misalignment problem is more severe for long optical paths necessary in a complicated optical setup. The breakdown of a large optical system into modules makes most of the optical paths short. The long necessary paths are completed with fiber optics. The modular approach also makes the system maintain

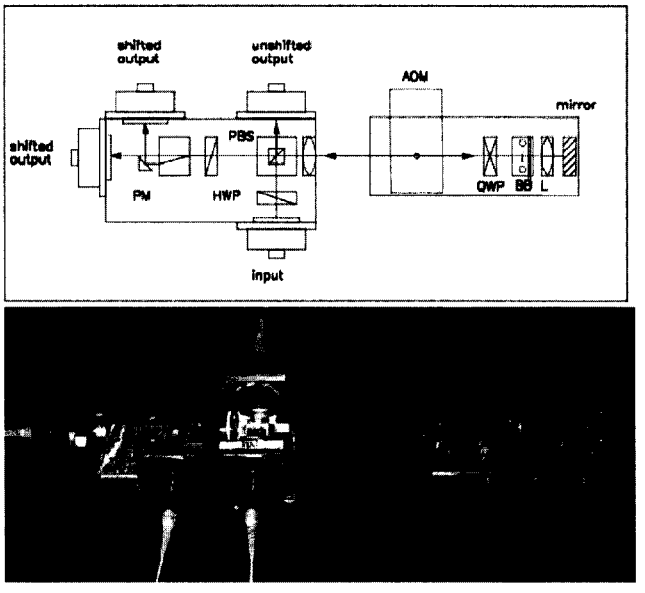

Fig. 5. A frequency shifter module with two shifted output ports and one unshifted port for the modules down the chain. (a) is the schematic design of the module and (b) is the figure of its actual implementation. The module is bolted down to a solid base when installed.

the flexibility. This flexibility is needed in the stage of the low TRL development. The modules can be eventually "potted" with epoxy. With the fiber pigtails, they are much like the pigtailed modules in telecommunication system.

The Cs atom experiment requires two main optical frequencies. These two frequencies are generated from two master lasers. The master lasers are frequency-stabilized to the corresponding Cs atomic transitions. The stabilized lasers are then frequency-shifted to obtain a tunable range of frequencies. These frequency-shifted laser beams are further "power-amplified" with multiple injection-locked slave lasers. The high power laser beams are then split and sent to different experiment ports. Therefore, the entire laser system can be made up with the following optical modules: master lasers, frequency lock modules, frequency shifters, slave lasers, and beam splitter/combiners.

Fig. 5 shows one example of the optical module design and its implementation. The module uses commercially available optical bench parts [12]. According to the vendor, the optical benches made of these parts maintain its optical alignment within 0.1 dB change in the temperature range of $-20°$C to 70°C. They also can survive 4 g shock. We have done some temperature cycling with our more complicated modules from 25°C to 35°C and found that the alignment has kept within $\pm 1.5\%$ in the output stability. The fiber coupling efficiencies in these modules typically range from 70% to 85%. The particular module shown in Fig. 5 is a frequency shifter using a double pass acousto-optic modulator (AOM). The double-pass configuration significantly increases the frequency tuning bandwidth. With the 80 MHz center frequency, the (half power) bandwidth with the fiber-in and fiber-out is 80 MHz. Though the module is made of two commercially available benches, they are bolted down together on a solid base when

installed to ensure rigidity. Later modules also used custom-made single stainless steel bases. The entire modular laser system consists of more than twenty such modules to deliver all necessary laser beams to two atom interferometers for atom trapping and cooling, state preparation and detection, and finally to realize the atom interferometers.

Polarization-maintaining (PM) fibers are used exclusively in this system to preserve the polarization of the laser beams. This makes the alignment of the polarization of the launch beam to the fiber axis critical. Care was taken whenever possible to launch the light into the fibers with pure linear polarization. In addition, polarizers are also placed at the output of the fibers to clean up any polarization-mode crosstalk inside the fibers. These steps are necessary because polarizating beam splitters (PBS) are extensively used to distribute the laser beams. Any polarization change will result in fluctuations in laser intensity. With all this precautions, the final laser intensity instability can only be kept within 2% level. The fiber-to-fiber coupling with FC/APC connectors tends to be lossy. These PM fiber related issues seem to be the main limitation of the system and need to be further addressed for future flight system.

C. Laser frequency and phase locking

There are effectively two laser subsystems in the implementation of atom interferometer of cold atoms; the MOT lasers that are used for trapping, cooling, and detection, and the Raman lasers that are used for splitting and recombining the atom waves through the Raman process. Each of these has specific requirement of frequency stability. Therefore, these lasers are actively frequency or phase locked. This section describes their implementations.

1) Master laser frequency stabilization: All laser frequencies are derived from master lasers. The free running laser has more than 1 MHz linewidth and drifts tens of MHz over time. It must be frequency-locked to a stable frequency reference. It is done by locking the laser to an atomic transition. Since we are interested in the transitions in Cs atom, it is most convenient to lock the laser to a nearby Cs resonance transition line.

In a Cs vapor cell, all transition lines are Doppler-broadened with unresolved lines. Therefore, saturation spectroscopy is employed to obtain the narrow natural linewidth. In the saturation scheme, a probe laser beam and a pump laser beam are counter-propagating through the cell. Only one velocity group of atoms will interact with both laser beams at the same time, thus achieving the sub-Doppler linewidth. To generate the necessary frequency error signal, we use the frequency modulation transfer scheme wherein the pump laser is frequency-modulated with AOM [13]. The setup is schematically shown in Fig. 6 on a miniature module. An 80 MHz AOM is used for the frequency modulation. The modulation frequency is set at 500 kHz. The frequency error signal is recovered from the phase-sensitive detection. The error signal is then split into a fast loop to the laser current control and a slow loop to the laser PZT control. This double loop scheme is often used in laser stabilization to achieve both a wider overall locking bandwith and a large drift correction range. The overall locking bandwidth is estimated about 100 kHz.

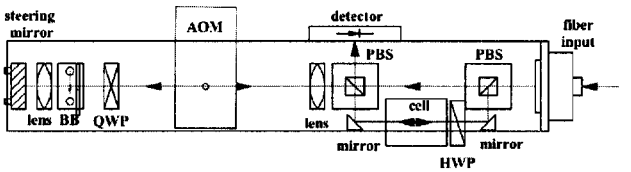

Fig. 6. The schematic of the saturation spectroscopy setup as implemented on a miniature optical module.

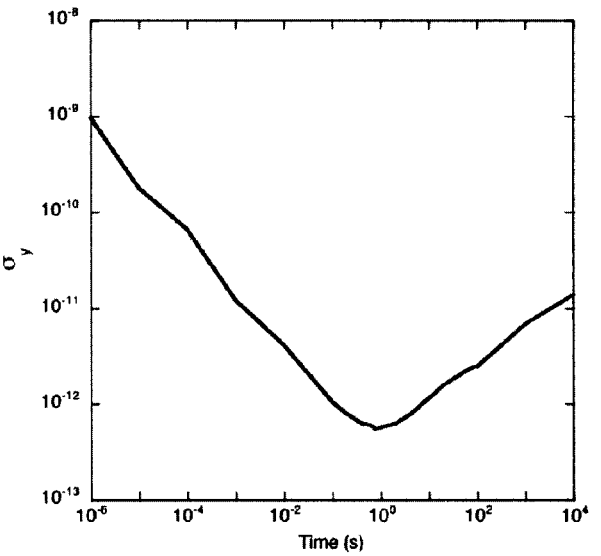

Fig. 7. Allan variance $\sigma(\tau)$ plot of the frequency locked master laser. The variance was obtained by measuring the beatnote of two identically locked lasers with a frequency counter.

To measure the long term stability of the locked master lasers, we compared the frequencies of two identically stabilized master lasers and measured the frequency difference against a stable rf source. Assuming the two laser fluctuations are not correlated, Fig. 7 plots the laser frequency stability in the Allan variance plot. The frequency stability goes down as $1/\sqrt{\tau}$ below 1 s, indicating a white frequency noise. The stability reaches 6×10^{-13} before going into the random walk regime. The demonstrated stability is sufficient for the atom interferometer operation. Nevertheless, we understand that the major source of the instability comes from the laser intensity fluctuation. Furthermore, there was no special environmental stabilization made to the cell. By resolving these technical issues, the long-term stability can be improved even further for other applications.

2) Raman laser phase locking: The atom interferometer is actually realized by a pair of counter-propagating laser beams as required by the stimulated Raman transitions [5]. In the Raman excitation process, the relative phase of the two Raman lasers is transferred to the atom wave. Therefore, the phase

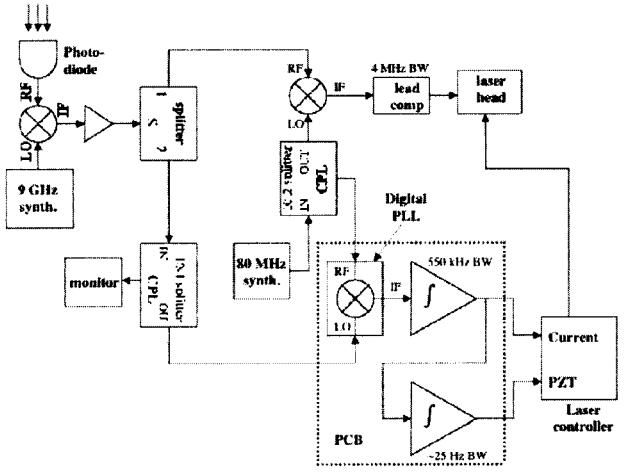

Fig. 8. The block diagram of the laser phase locking setup.

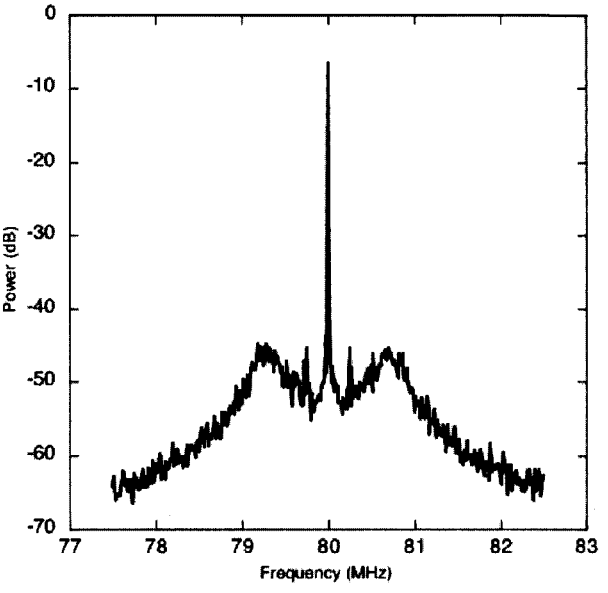

Fig. 9. The spectrum of the beatnote of the two phase locked lasers. The spectrum resolution is 1 kHz, limited by the spectrum analyzer, and the central peak contains 99% of the rf power.

fluctuation directly results in the atom interferometer fringe noises. There are a number of ways to generate the phase-coherent laser pairs. We will be using the direct phase locking of one laser to another because it is simple, versatile and most suitable for a space-borne system.

The basic implementation of the laser phase locking is through a phase locking loop (PLL). The relative phase of the two lasers is detected by mixing the two laser fields in a fast photodetector. This beatnote is mixed down to the baseband frequency, properly filtered, and fed back to one of the laser frequency actuator. Fig. 8 shows the phase locking loop diagram of our implementation. The laser beatnote is at 9.2 GHz, the frequency offset required by the Cs hyperfine splitting. This beatnote is first mixed down to an intermediate frequency of 80 MHz. At this intermediate frequency, one can use a digital PLL device which not only provides the necessary phase discrimination but also frequency discrimination at large frequency difference, which offers a large frequency acquisition and locking range. An analog phase detector is also used in parallel for increased loop bandwidth. While this phase error is directly fed into the high frequency current modulation port of the laser, the digital PLL signal is further integrated and goes to the lower frequency modulation ports. The further integration of the low frequency signal increases near DC gain of the loop and ensures the true phase locking against step error signals.

This PLL gives a robust phase locking of the two lasers. Fig. 9 shows the beatnote spectrum of the two lasers. The central peak contains 99% of the total rf power. Its width is only limited by the spectrum analyzer resolution. The rms phase noise is less than 0.1 rad.

We should also point out that, in our experimental setup, we are not locking the master lasers directly. Instead, we take the beatnote measurement right before the laser pulse switches, but after all additional fiber connections, slave lasers, and frequency shifters. Therefore, any subsequently induced phase noises will be detected and corrected by the PLL.

IV. Conclusion

An atom interferometer-based gravity gradiometer holds great promise for the Earth Sciences in geodesy, solid earth modelling, and climate and resource observation. Our goal is to develop a space-borne atom interferometer system. Towards that end, we are currently implementing a laboratory version of the gravity gradiometer. Tremendous progress has been made in developing the system at the component level. We have reported here the successful development of a compact cold atom source, a robust modularized laser and optics system, and the implementations of laser frequency and phase lockings.

Acknowledgment

This research was carried out at the Jet Propulsion Laboratory, California Institute of Technology, under a contract with the National Aeronautics and Space Administration.

References

[1] http://www.csr.utexas.edu/grace/.
[2] http://www.esa.int/export/esaLP/goce.html
[3] http://www.physics.umd.edu/GRE/SGGs.htm
[4] M. Kasevich and S. Chu, "Measurement of the gravitational acceleration of an atom with a light-pulsed atom interferometer," Appl. Phys. B **54**, 321 (1992).
[5] M. Kasevich and S. Chu, "Atomic interferometry using stimulated Raman transitions," Phys. Rev. Lett. **67**, 181–184 (1991); Ch. J. Bordé, "Atomic interferometry with internal state labeling," Phys. Lett. A **140**, 10–12 (1989).
[6] Ch. J. Bordé, C. R. Acad. Sci. Paris T. 2, S. IV 509–530 (2001).

[7] N. Yu, J. M. Kohel, L. Romans and L. Maleki, "Quantum gravity gradiometer sensor for earth science applications," ESTC 2002, Pasadena, CA (2002).
[8] G. Santarelli *et al.*, "Quantum projection noise in an atomic fountain: A high stability cesium frequency standard," Phys. Rev. Lett. **82**, 4619 (1999); J. M. McGuirk *et al.*, "Low-noise detection of ultra-cold atoms," Opt. Lett. **26**, 364 (2001).
[9] J. M. McGuirk, G. T. Foster, J. B. Fixler, M. J. Snadden and Mark Kasevich, "Sensitive absolute gravity gradiometry using atom interferometry," Phys. Rev. A **65**, 033608 (2002).
[10] K. Dieckmann, R. J. C. Spreeuw, M. Weidemüller and J. T. M. Walraven, "Two-dimensional magneto-optical trap as a source of slow atoms," Phys. Rev. A **58**, 3891–3895 (1998); J. Schoser, A. Batär, R. Löw, V. Schweikhard, A. Grabowski, Yu. B. Ovchinnikov and T. Pfau, "An intense source of cold Rb atoms from a pure two-dimensional magneto-optical trap," Phys. Rev. A **66**, 023410 (2002).
[11] J. Ramirez-Serrano *et al.* "A compact multi-stage 2D-MOT atom source," to be published.
[12] Optics For Research, Inc., Caldwell, New Jersey 07006.
[13] J. H. Shirley, "Modulation transfer processes in optical heterodyne saturation spectroscopy," Opt. Lett. **7**, 537–539 (1982).